Mechanisms of the Aqueous Solvolysis of the Ring-opening of the Lactone Ring of Goniodomin A

B. Andes Hess Jr. [a*] and Lidia Smentek [a]

[a] Department of Chemistry, Vanderbilt University, Nashville, Tennessee 37235, USA.

Authors' contributions

This work was carried out in collaboration between both authors. Both authors read and approved the final manuscript.

Short Communication

ABSTRACT

The phycotoxin Goniodomin A is a Dinoflagellate of the Alexandrium genus and is a macrocyclic lactone. It is found widely in sea water and is known to open slowly the lactone in water. The cleavage of the lactone is sensitive to the pH of the water. As one changes the pH from ~6 to 8 its solvolytic rate dramatically increases. Treatment of kinetic data previously published indicates that there are two competing first-order reactions, an S_N1 and an intramolecular S_N2, which is a pseudo first-order reaction.
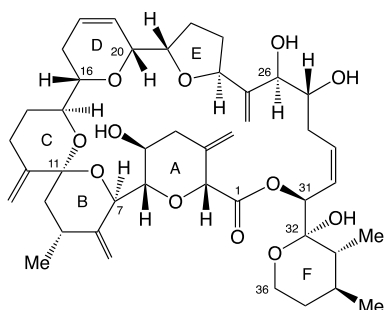
_____

Corresponding author: E-mail: b.andes.hess @vanderbilt.edu;

1. INTRODUCTION

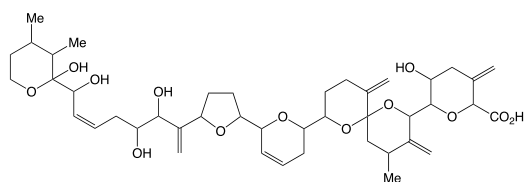Dinoflagellate of the Alexandrium genus (GDA) is produced by four species of the genus - *hiranoi, A. pseudogonyaulax, A. monilatum* and *A. taylorii.* [1-4]. Murakami and Takeda determined the structure of GDA [1,5], which was recently confirmed by X-ray crystallography [6]. GDA is a polyketide macrolide containing six oxygen heterocycles, five macrocyclic rings with two of them constituting spiro ketals. The sixth ring contains a hemiketal, which will be the focus of this presentation.

In 2020 Onofrio reported that GDA degrades in pure water at pH 7, and significantly faster in sea water where the pH is approximately 8 [7]. Further studies by Hintze [8] found that the rate of degradation of GDA (1) in deionized water (~pH 6.5), Milli-Q water (pH 7.2), and in culture medium (pH 8.2) became significantly faster with increase of the pH.

Chemical Structure 1. GDA (1)

The product of the degradation is a carboxylic acid like the seco acid of GDA (2). One might expect the reaction to proceed simply with hydrolysis of the lactone.

Chemical Structure 2. GDA-SA (2)

However, an alternative mechanism would be that of solvolysis with the leaving group being the carboxylate anion with production of a carbocation at C_{31}. While the carboxylate is one of the worst known leaving groups in nucleophilic substitutions, there are two aspects of the structure of GDA (1), which might make the solvolytic mechanism the preferred one. The first is that the forming carbocation is allylic since the developing positive charge on C_{31} is allylic. The second one is that the OH group at C_{32} might interact as a neighboring group in which case an epoxide would be formed; or the epoxide might simply exist on the concerted reaction pathway. In the latter case it would not form the C_{31} carbocation but rather the C_{32} carbocation, which would be stabilized by the lone pair of the ether oxygen. The solvolytic degradation of GDA (1) was confirmed by Harris with $H_2^{18}O$ [9].

This study treats computationally a model system to determine the solvolytic mechanism. The dramatic change in rate vs pH found by Hintze [8] suggests that there might be two competing mechanisms, as mentioned above.

2. KINETICS OF THE SOVOLYTIC REACTIONS

Hintze studied the degradation of GDA (1) at three different pH values. Included in his thesis were the plots of kinetic data (concentration vs. time in days). It was found that these kinetic data all arose from first order reactions – straight lines were found when plotting the natural log of the concentration at time t divided by the initial concentration (t=0). Our kinetic treatment of these data are presented in Fig. 1.

The $t_{1/2,}$ half-lives, of these three kinetic treatments are 3.4, 2.0 and 1.2 days, respectively. The dramatic change in $t_{1/2}$ lives suggests that there might be two competing first-order reactions occurring, one being dominant at pH 6 and the other at pH 8. What is the difference between these two pH values? Given that both are likely nucleophilic substitutions, it is possible that the hydroxide ion might be involved in the major reaction occurring at pH 8, since the hydroxide concentration is two orders of magnitude higher at pH 8 than at pH 6. At this point it was possible that the dominant reaction at pH 6 is S_N1 and at pH 8 S_N2. The calculations described below were done to confirm this proposal.
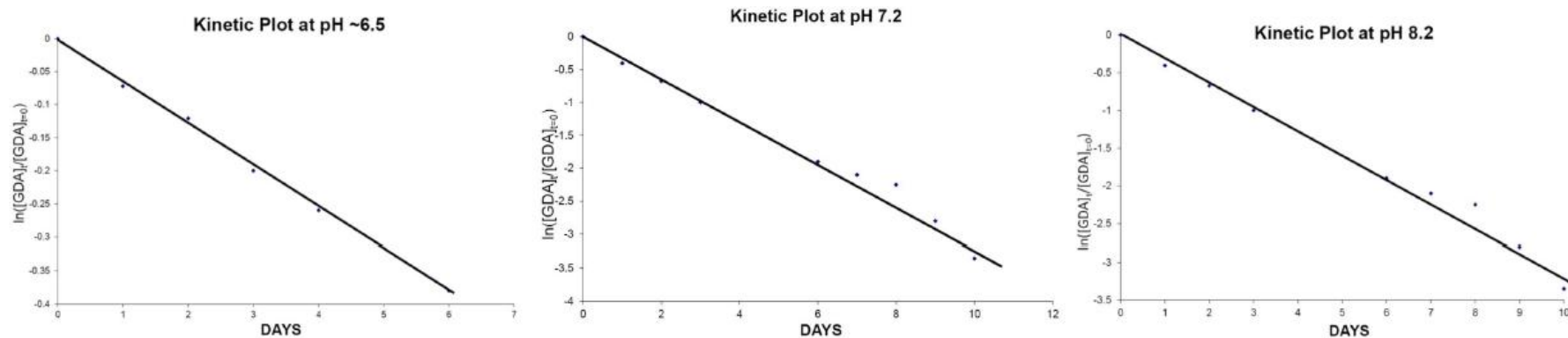
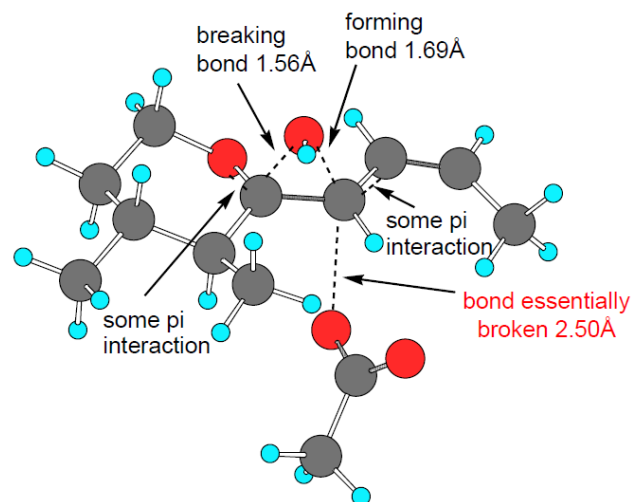**Fig. 1. The kinetically treated data of Hintze [8] at pH ~6.5, 7.2 and 8.2**

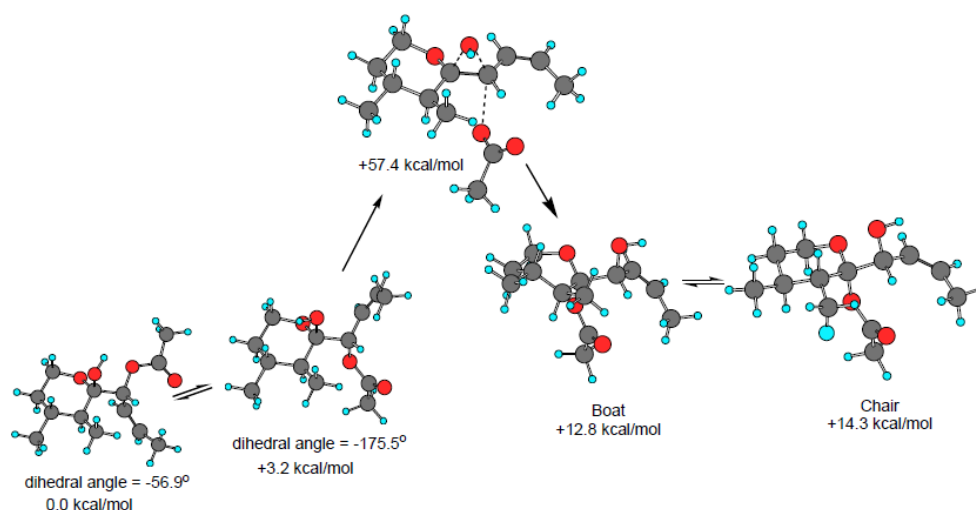**Fig. 2. The concerted, but asynchronous, transition structure for the S_N1 reaction dominant at pH 6**

Fig. 3. The computed concerted reaction pathway for the S_N1 reaction dominant at pH 6

3. DFT CALCULATIONS

The calculations [10] described below were done to explain the proposal based on the kinetic results. At pH 6 an S_N1 reaction occurs with a unimolecular ionization with the carboxylate acting as the leaving group. Using the model system mentioned above a transition structure (Fig. 2) was located, which suggested a concerted rearrangement with the forming carbocation. As seen the ionization is assisted by the double bond attached to C_{31} as well as migration of the OH group from C_{32} to C_{31} and is further stabilized by interaction of the hemiacetal oxygen attached to C_{32}. The latter is crucial in stabilizing the final rearranged carbocation. Intrinsic Reaction Coordinate (IRC) calculations produced the reactant and product as shown in Fig. 3. In the case of the reactant the IRC gave a conformer of that in the x-ray structure [6].

The IRC reactant conformer has a dihedral angle of the two carbons connecting the acyclic chain to the carboxylate carbon of the lactone of -175.5° and dihedral angle of its conformer is -56.9°. The x-ray conformer has a dihedral angle that would prevent OH group participation in the concerted reaction. The IRC gave a product with the six-membered ring in a boat conformation. Interestingly, its chair conformer was higher in energy than that of the boat conformer.

DFT (Density Functional Theory) calculations were carried out in a water medium, however, S_N1 reactions are not accurately described by these calculations [11]. It is known that during such reactions at first it forms a contact ion pair,

which in turn forms a solvent separated ion pair. With this type of calculation, these ion pairs are not well described, and the leaving group has only one choice, that is to collapse to the newly formed carbocation produced by the concerted reaction. The activation energy is also large, since while the calculation is modeled with a surrounding solvent of water, no water molecules are present in the vicinity of the ionization of the C-O bond to "assist" in the ionization, leading to the formation of the solvent separated ion pair. Consequently, the computed activation energy is much higher than the experimental one.

However, it is possible to obtain a better estimate of the overall energetics of carbocation reactions by carrying out calculations on the formed carbocation. There is good evidence for this in recent computations of carbocation rearrangements in terpene chemistry [12]. Beginning with the carbocation that is formed by loss of the carboxylate group in our model system a transition structure (Fig. 4) was located remarkably like that presented above (Fig. 2).

More dramatic is the difference in the overall energetics of the carbocation reaction in Fig. 5 than that in Fig. 3. Note the exceptionally low activation energy (+4.0 kcal/mol), and the overall energy of reaction between the reactant and the IRC product is -14.5 kcal/mole. It is apparent that the major driving force for this concerted rearrangement is the ability of the ether oxygen in the oxane ring to stabilize the carbocation on C_{32}. This is not unexpected given that the methoxy group has a large negative Hammett σ_{para} constant.
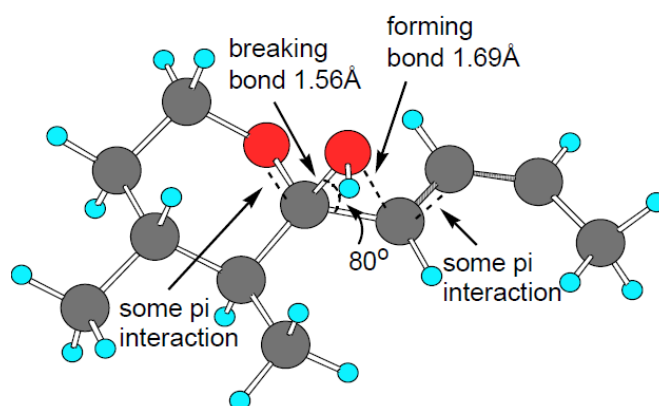
Fig. 4. The S$_N$1 transition structure (with an overall positive charge) located for the model system carbocation
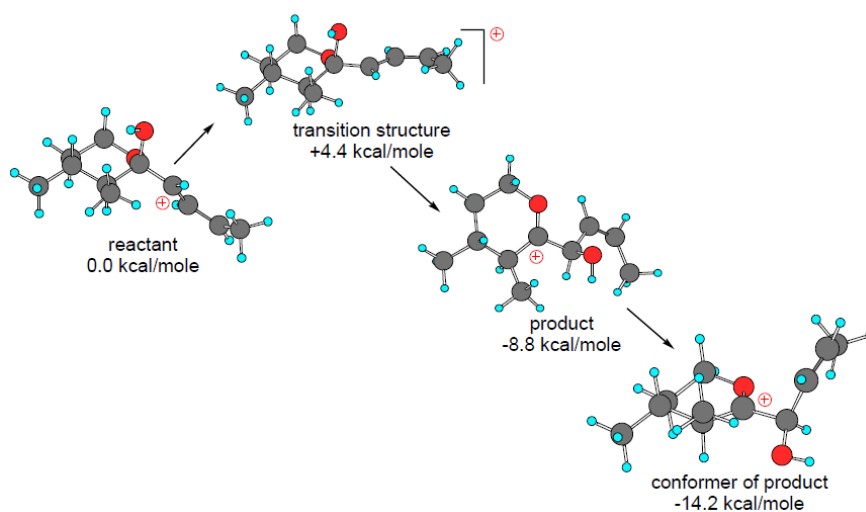

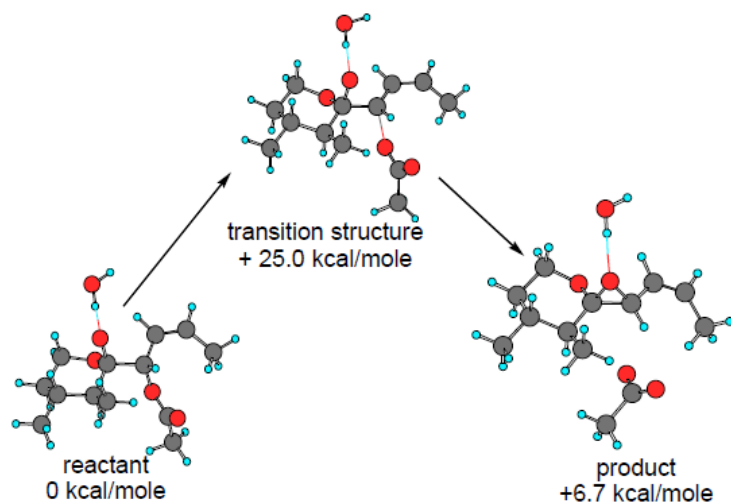**Fig. 5. The overall DFT pathway of the carbocation in the S$_N$1 reaction dominant at pH 6**

Fig. 6. The reaction pathway which includes a hydroxide ion of the solvolysis of the ester at pH 8 or under basic conditions
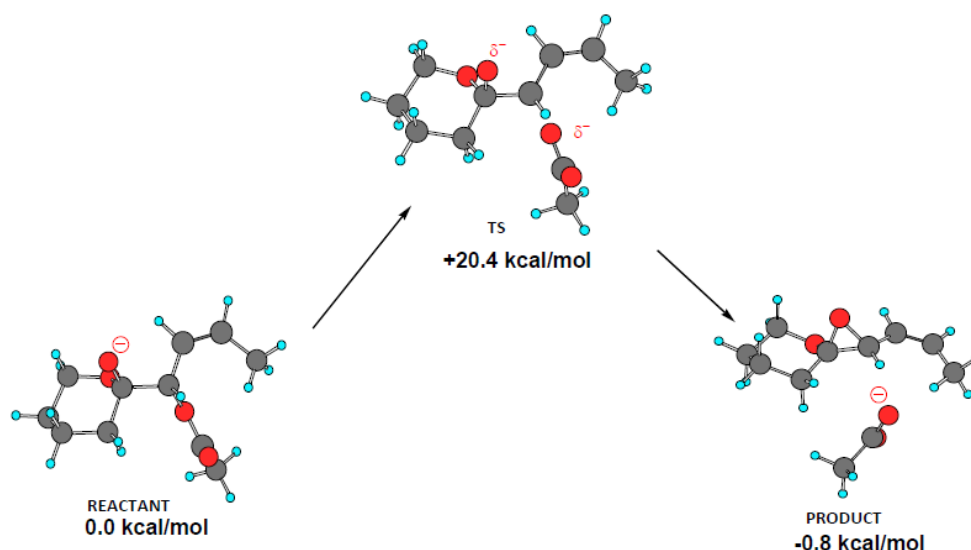
13

Fig. 7. The S_N2 reaction at pH 8 beginning with the proton removed from the oxygen at C_{32}

Turning to the dominant reaction at pH 8, a DFT study was conducted with the addition of a hydroxide ion. A transition structure was located (Fig. 6) for removing the hydrogen from the OH group on C32. IRC calculations gave the reaction pathway shown in Fig. 6.

Again, the overall reaction studied in the modeled water solution suffers from no individual water molecules present near the structures along the reaction pathway. For example, the carboxylate leaving group would be hydrated with water molecules, which would change the energy of the reaction. The pathway was also studied beginning with the anion of the reactant (Fig. 7). This reaction is indeed an intramolecular S_N2 reaction. In this case the attacking nucleus is the negatively charged oxygen on C_{32}. While the overall reaction energy is now negative, it is small at -0.8 kcal/mol. Again, the energetics are different from what one would expect experimentally because of lack of water molecules interacting with the structures along the reaction pathway.

4. DISCUSSION

The study revealed that treatment of the kinetic data shown in Fig. 1 shows a dramatic increase in $t_{1/2}$ as pH is increased and is highly likely a result of two competing first order reactions, both of which have a dependence on pH. At the lower pH the reaction is a typical S_N1 reaction with a neighboring group participation of the OH group on the carbon adjacent to the developing positive

charge that is produced by the leaving group. The driving force of this is the formation of the positive charge on the adjacent carbon (Fig. 5), which is stabilized by the oxane oxygen by participation of its unshared pair of electrons.

At higher pH the second reaction becomes dominant because of the increase in hydroxide ion concentration, which acting as a base, removes the proton from the OH (see Fig. 6) allowing the formation of the epoxide. In this reaction the rate determining step involves two reactants. Note that one reactant is the hydroxide ion, whose concentration is constant during the reaction. Hence this is simply a pseudo first-order reaction since the *change* in the concentration of the substrate is far higher than that of the hydroxide. Hence, the kinetic treatment shows two competing first order reactions, but as seen from the calculations, the one at higher pH is a pseudo-first order reaction.

Whether or not the epoxide is stable under the basic reaction conditions is an interesting question. It has two pathways that ring opening of the epoxide can occur as shown in Fig. 8, with the two products being diastereomers. In addition, the product giving rise to the *R-R* one favored because of steric hindrance at the carbon undergoing the nucleophilic attack. Interestingly the S_N1 reaction would also give rise to a C_{31} *S* -C_{32} *S* glycol. However, under the aqueous conditions, the C_{32} carbon might be racemized by mutarotation of the hemiketal.

C_{31}-*R* C_{32}-*R*
the less hindered backside attack

C_{31}-*S* C_{32}-*S*

C_{31}-*S* C_{32}-*S*
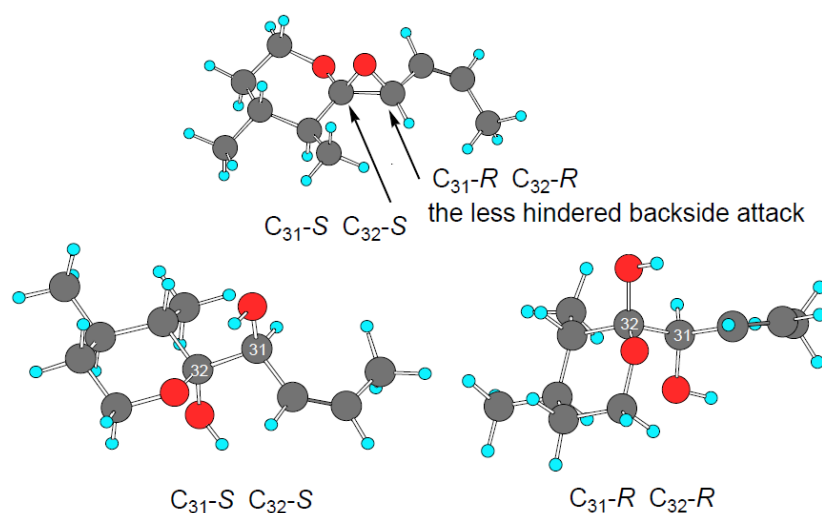
C_{31}-*R* C_{32}-*R*

Fig. 8. Potential products of base catalyzed opening of the epoxide

5. CONCLUSIONS

The DFT results suggest that indeed there might be in the ring-opening of the lactone competing first-order nucleophilic substitution reactions. At the lower pH the S_N1 dominates and at higher pH an intramolecular S_N2 reaction is predicted to dominate as a pseudo first-order reaction.

SUPPLEMENTARY MATERIALS

Supplementary materials available in this link: https://journalirjpac.com/index.php/IRJPAC/libraryFiles/downloadPublic/20.

COMPETING INTERESTS

Authors have declared that no competing interests exist.

REFERENCES

1. Murakami M, Makabe M, Yamaguchi K, Konosu S, Wälchli W. Goniodomin a, a novel polyether macrolide from the dinoflagellate *Goniodoma pseudogoniaulax.* Tetrahedron Lett. 1998; 29:114-52.
2. Hsia MH, Morton SL, Smith LL, KR. Beacuchesne KR, Huncik KM, Moeller PDR. Production of goniodomin A by the planktonic, chain-forming dinoflagellate *Alexandrium monilatum* (Howell) Balech isolated from the Gulf Coast of the United States. Harmful Algae. 2006;(5):290-9.
3. Triki HZ, Laabir M, Moeller P, Chomérat N, Daly-Yahia OK. First report of goniodomin A production by the dinoflagellate *Alexandrium pseudogonyaulax* developing in southern Mediterranean (Bizerte Lagoon, Tunisia) Toxicon. 2016;111: 91-9.
4. Mertens KN, Adachi M, Anderson DM, Band-Schmidt CH, Bravo I, Brosnahan ML et al. Morphological and phylogenetic data do not support the split of Alexandrium into four genera. Harmful Algae. 2020; 98:101902.
5. Takeda Y. Shi J, Oikawa M, Sasaki M. Assignment of the Absolute Configuration of Goniodomin A by NMR spectroscopy and Synthesis of Model Compounds. Org. Lett. 2008;10(5):1013–6.
6. Tainter CJ, Schley ND, Harris CM, Stec DF, Song AK, Balinski A et al. Algal Toxin Goniodomin Binds Potassium Ion Selectively to Yield a Conformationally Altered Complex with Potential Biological Consequences. J. Nat. Prod. 2020;83: 1069-81.
7. Onofrio MD, Mallet CR, Place AR, Smith JL. A screening tool for the direct analysis of marine and freshwater phycotoxins in organic SPATT extracts from the Chesapeake Bay. Toxins. 2020;12:322-38.
8. Hintze L, Master Thesis. University of Applied Sciences. Mannheim; 2021.
9. Harris TM. Private Communication.
10. (a) All calculations were performed with Gaussian 09 (RevisionA.02). Frisch M, Trucks GW; Schlegel HB; Scuseria GE, Robb MA; Cheeseman JR et al. Gaussian Inc. Wallingford CT.
(b) Geometries were optimized without symmetry constraints using M06-2X/6-31G*; 2009. Wang Y, Verma P, Jin X, Truhlar DG, He X.

(c) Revised M06 density functional for main-group and transition-metal chemistry. Proc. Natl. Acad. Sci. U. S .A. 2018;115: 10257-62. Zhao Y, Truhlar DG. Theor. Cheim. Acta; 2008.

(d) All structures were characterized by frequency calculations and reported energies include zero-point energy corrections (unscaled). Intrinsic reaction coordinate (IRC) calculations. Gonzalez C, Schlegel HB. Reaction path following in mass-weighted internal coordinates. J. Phys. Chem. 1990; 94:5523–27.

(e) Frequency calculations were also used to characterize transition Structures. Fukui K. The path of chemical reactions-the IRC approach. Acc. Chem. Res. 1981;14: 363–8.

11. Otomo T, Suzuki H, Lida R, Takayanagi T. S_N1 reaction mechanisms of *tert*-butyl chloride in aqueous solution: What can be learned from reaction path search calculations and trajectory calculations for small hydrated clusters? Comp Theor. Chem. 2021;1201: 113278-85.

12. (a) Smentek L, Hess Jr. BA. Compelling Computational Evidence for the Concerted Cyclization of the ABC Rings of Hopene from Protonated Squalene. J. Am. Chem. Soc. 2010;132:17111-7.

(b) Hess Jr. BA, Smentek L. The concerted nature of the cyclization of squalene oxide to the protosterol cation. Angew. Chem. Int. Ed. 2013;52:11029-33.

(c) N. Chen S. Wang L. Smentek BA. Hess Jr. R. Wu. Biosynthetic Mechanism of Lanosterol: Cyclization. Angew. Chem. Int. Ed. 2015;54:8693-8696.

(d) Matsuda SPT, Wilson WK, Xiong Q. Mechanistic insights into triterpene synthesis from quantum mechanical calculations. Detection of systematic errors in B3LYP cyclization energies. Org. Biomol. Chem. 2006;4:530-543.

(e) Tantillo TJ. Biosynthesis *via* carbocations: Theoretical studies on terpene formation. Nat. Prod. Rep. 2011; 28:1035-53.

(f) Hong YJ, Tantillo TJ. Which Is More Likely in Trichodiene Biosynthesis: Hydride or Proton Transfer? Org. Lett. 2006;8:4601-4.

(g) Hong YJ, Tantillo TJ. Consequences of Conformational Preorganization in Sesquiterpene Biosynthesis: Theoretical Studies on the Formation of the Bisabolene, Curcumene, Acoradiene, Zizaene, Cedrene, Duprezianene, and Sesquithuriferol Sesquiterpenes. J. Am. Chem. Soc. 2009; 131:7999-8015.

_____

Peer-review history:
The peer review history for this paper can be accessed here:
https://www.sdiarticle5.com/review-history/94100